

Laboratory-Prostate cancer  
Antitumor effect of a dual cancer-specific oncolytic adenovirus  
on prostate cancer PC-3 cells

Chuan-xin Cui, Ph.D.<sup>a,b</sup>, Yi-quan Li, Ph.D.<sup>b,c</sup>, Yu-jia Sun, M.S.<sup>d</sup>, Yi-long Zhu, Ph.D.<sup>b,c</sup>,  
Jin-bo Fang, Ph.D.<sup>b,c</sup>, Bing Bai, M.S.<sup>b,c</sup>, Wen-jie Li, Ph.D.<sup>b,e</sup>, Shan-zhi Li, M.S.<sup>b,c</sup>,  
Yi-zhen Ma, M.S.<sup>b,e</sup>, Xiao Li, Ph.D.<sup>b,c,e,\*</sup>, Wei-hua Wang, Ph.D.<sup>a,f,\*</sup>, Ning-yi Jin, Ph.D.<sup>b,c,e,\*</sup>

<sup>a</sup> Department of Dermatology, China-Japan Union Hospital of Jilin University, Changchun, Jilin, P. R. China

<sup>b</sup> Institute of Military Veterinary Medicine, Academy of Military Medical Science, Changchun, P. R. China

<sup>c</sup> Changchun University of Chinese Medicine, Changchun, P. R. China

<sup>d</sup> Department of Operating Room, The Second Hospital of Jilin University, Changchun, Jilin, P. R. China

<sup>e</sup> Jiang su Co-innovation Center for Prevention and Control of Important Animal Infectious Diseases and Zoonoses, Yangzhou, P. R. China

<sup>f</sup> Department of Urology Surgery, China-Japan Union Hospital of Jilin University, Changchun, Jilin, P. R. China

Received 16 October 2018; received in revised form 21 November 2018; accepted 16 December 2018

## Abstract

**Purpose:** Apoptin can specifically kill cancer cells but has no toxicity to normal cells. Human telomerase reverse transcriptase (hTERT) acts as a tumor-specific promoter, triggering certain genes to replicate or express only in tumor cells, conferring specific replication and killing abilities. This study aimed to investigate the anticancer potential of the recombinant adenovirus Ad-apoptin-hTERTp-E1a (Ad-VT) in prostate cancer.

**Methods:** The pGL4.51 plasmid was used to transfect PC-3 cells to construct tumor cells stably expressing luciferase (PC-3-luc). Crystal violet staining and MTS assays determined the ability of Ad-VT to inhibit cell proliferation. Ad-VT-induced apoptosis of PC-3-luc cells was detected using Hoechst, Annexin V, JC-1 staining, and caspases activity analysis. PC-3-luc cells invasion and migration were detected using cell-scratch and Transwell assays. In vivo tumor inhibition was detected using imaging techniques.

**Results:** Crystal violet staining and MTS results showed that the proliferation ability of PC-3-luc cells decreased significantly. Hoechst, JC-1, and Annexin V experiments demonstrated that Ad-VT mainly induced apoptosis to inhibit PC-3-luc cell proliferation. Ad-VT could significantly inhibit the migration and invasion of PC-3-luc cells over a short period of time. In vivo, Ad-VT could effectively inhibit tumor growth and prolong survival of the mice.

**Conclusions:** The recombinant adenovirus, comprising the apoptin protein and the hTERTp promoter, was able to inhibit the growth of prostate cancer PC-3 cells and promote their apoptosis. © 2018 Elsevier Inc. All rights reserved.

**Keywords:** Apoptin; hTERT; Recombinant adenovirus; PC-3-luc cells

## 1. Introduction

Prostate cancer is the most common malignant tumor of the male genitourinary system. It is an epithelial malignant tumor [1], and has a high morbidity and mortality [2–4]. Prostate cancer is the most common malignant tumor of the male genitourinary system. It is a malignant epithelial tumor, with high morbidity and mortality rates. In United States, most commonly diagnosed cancer in men is prostate

cancer, with newly 161,360 people were diagnosed in 2017 [5,6]. In recent years, the incidence of prostate cancer in China has significantly increased. Prostate cancer has become one of the malignancies that threaten men worldwide [7]. Currently, the treatment options for prostate cancer are including surgery, combinatorial chemotherapy, immunotherapy, and radiotherapy. However, these treatment options have significant limitations such as low curative effect, causing large necrotic areas, and serious side effects. In addition, there is no targetable drug presented in clinics. The hotspot of current research in prostate cancer is to find better effective drugs with low side-effects.

\*Corresponding authors. Tel: +86-0431-86985923; fax: +86-0431-87985861.

E-mail addresses: [lixiao06@mails.jlu.edu.cn](mailto:lixiao06@mails.jlu.edu.cn) (X. Li),  
[wangweihuajilin@163.com](mailto:wangweihuajilin@163.com) (W.-h. Wang), [skylee6226@163.com](mailto:skylee6226@163.com) (N.-y. Jin).

By the widespread usage of genetic engineering in biology and in medicine, gene targeted therapies have become possible for cancer management. Gene therapy has shown prominent advantage, and the study found that the virus has great potential in cancer treatment [8]. Oncolytic virus therapy is an oncolytic virus that has the function of targeting and killing tumor cells by selecting some strains with weak pathogenicity in nature or by objective genetic modification of certain viruses [9]. At present, there are dozens of oncolytic viruses for tumor treatment, including adenovirus, type I simple herpes virus, Newcastle disease virus, vaccinia virus, reovirus, and vesicular stomatitis virus [10]. The treatment using adenovirus as a carrier to target cancer cells, has received extensive research attention and has become a research hotspot. Adenovirus therapy is expected to replace traditional therapy for cancer treatment [11,12]. However, it is critical to track and monitor changes of genes and cells during the treatment. Molecular imaging has emerged as a technology that effectively track and monitor genes and cells during treatment [13,14].

Bioluminescent imaging (BLI) is a visualization technique for tracing cells and tissue, and gene behavior in vivo [15]. BLI is characterized by light scattering and has unique imaging advantages. In addition, tissue and cells have almost no endogenous luminescence and low endogenous signal-to-noise ratio; therefore, background interference can be effectively eliminated, and the bioluminescence signal in complex organisms can be clearly observed [16]. With the rapid development of in vivo BLI technology, it has been widely used in research into various types of cancer, and has become a promising tool in the field of biomedicine. The luciferase gene is used as a reporter gene for in vivo bioluminescence imaging. The firefly luciferase gene is the most widely used and has high sensitivity, low endogenous, and good stability. It is often used to label viruses, bacteria, and tumor cells [17]. The establishment of a luciferase-labeled animal tumor model enables the visual, real-time, and continuous monitoring of the growth and metastasis of tumor cells in different tumor models, such as in situ tumors, metastatic tumors, and spontaneous tumors. Even subtle changes can be detected in a timely manner, thus BLI provides an ideal animal model for a more intuitive evaluation of the therapeutic effects of anticancer drugs [18].

Apoptin was originally identified as an apoptosis-inducing protein derived from Chicken Anemia Virus (CAV), a single-stranded DNA virus of the Gyrovirus genus [19]. The CAV genome contains three partially overlapping open reading frames encoding viral proteins from a single polycistronic mRNA: VP1 (capsid protein), VP2 (protein phosphatase, scaffold protein) and the death inducing protein VP3 [20]. Expression of VP3 alone was shown to be sufficient to trigger cell death in chicken lymphoblastoid T-cells and myeloid cells, but not in chicken fibroblasts, and it was therefore renamed apoptin [21]. The gene encoding apoptin was among the first tumor selective anticancer genes to be isolated, and has become a focus in cancer research because

of its ability to induce apoptosis in a variety of human tumor cells, including melanoma, lymphoma, colon carcinoma, and lung cancer, while leaving normal cells relatively unharmed [22–25]. Thus, apoptin seems to sense an early event of oncogenic transformation and induces cancer-specific apoptosis, regardless of tumor type; thus, it represents a potential future anticancer therapeutic agent.

Transcription of human telomerase reverse transcriptase (hTERT) is a major step in regulating telomerase activity [26]. Embryonic stem cells and induced pluripotent stem cells maintain their telomere length by expressing telomerase. The expression of telomerase is also upregulated in 85% to 90% of malignant tumor cells, giving them unlimited proliferation ability. Thus, telomerase is essential for cancer cells to maintain their immortality. Therefore, by interfering with the telomerase enzyme activity, the growth of cancer cells can be inhibited [27–29]. The *hTERT* promoter is inactive in most normal cells, but exhibits high activity in many human cancers. In many studies, the high expression of a protein targeting tumor cells is also dependent on the high efficiency and specificity of the *hTERT* promoter, thus opening up new prospects for tumor therapy.

In a previous study, we exploited the characteristics of apoptin to construct a dual cancer-specific oncolytic adenovirus expressing apoptin (Ad-Apoptin-hTERTp-E1a, Ad-VT) [30], which allows adenovirus to specifically replicate in tumor cells, and enables the apoptin protein to be expressed in a large amounts in tumor cells, thereby effectively killing the tumor. We have demonstrated the remarkable tumor killing effect of the recombinant adenovirus in a variety of tumor cells [30–34].

In the present study, luciferase-labeled human prostate cancer cell line PC-3-luc was constructed, and through the detection of growth characteristics and cell cycle of PC-3-luc cells and PC-3 cells, we verified that there were no significant differences in biological characteristics between the 2 types of cells. Subsequently, a series of different in vitro experiments and the establishment of a luciferase labeled BALB/c nude mouse subcutaneous tumor model were used to study the inhibitory effect of recombinant adenovirus Ad-VT on tumors, which provided a theoretical basis for the treatment of prostate cancer using the oncolytic adenovirus Ad-VT.

## 2. Materials and methods

### 2.1. Cells, viruses and animals

PC-3 cells were cryopreserved cells purchased from the Shanghai Institute of Biology cell bank. PC-3 cells were maintained in Dulbecco's modified Eagle's medium (DMEM), with 10% fetal bovine serum, 1000 U/ml penicillin, and 100 U/ml streptomycin. All the reagents for cells culture were purchased from GE healthcare life sciences, Hyclone Laboratories, (Logan, UT).

Recombinant adenoviruses Ad-Apoptin-hTERTp-E1a (Ad-VT), Ad-hTERTp-E1a (Ad-T), Ad-Apoptin (Ad-vp3),

and Ad-mock were constructed and preserved in our laboratory (Laboratory of molecular Virology and Immunology, Military Medical Science Academy of the PLA, Changchun, China) (Fig. 1) [30]. The constructed shuttle plasmids were cotransfected into HEK-23 cells, and then a recombinant adenovirus was produced by homologous recombination. The virus was purified using an Adeno-X Virus Purification kit (BD Bioscience Clontech, San Diego, CA) and the virus titer was detected using an Adeno-X Rapid titer kit (BD Bioscience Clontech, San Diego, CA).

Female BALB/c nude mice aged 4 to 5 weeks were purchased from the Experimental Animal Center of the Academy of Military Medical Sciences of China. The animal experimental protocols were approved by the Institutional Animal Care and Use Committee of the Chinese Academy of Military Medical Science, Changchun, China (10ZDGG007). All surgery was performed under sodium pentobarbital anesthesia, and all efforts were made to minimize suffering.

## 2.2. Construction and identification of PC-3-luc cells

The PC-3 cells were cultured at  $2 \times 10^5$  cells/well in 6-well cell culture plates, and cultured at 37 °C in 5% CO<sub>2</sub> for 24 hours. Subsequently, the cells were transfected with a mixture of 4 μg pGL4.51 plasmid

(Promega, Madison, WI) and 4 μl of Effectene Transfection Reagent (QIAGEN, Beijing, China). After transfection for 24 hours, PC-3 cells were digested and adjusted to a density of 100 cells/well, and added to a new 6-well plate. At the same time, a certain concentration of geneticin (G418) was used for screening, and fresh medium was changed every 2 days. G418 was used until a single resistant clone appeared; the above well-grown clones were selected into 96-well plates at 100 μl/well, and the G418 (BD Bioscience Clontech, San Diego, CA) concentration was maintained. When the cell confluence reached 80% or more, the cells were transferred to 24-well plates and culture was continued. Similarly, when the cell confluence reached 80% or more, they were transferred to a 12-well plate and assayed for their luciferase activity.

The preliminary screened cell clones were cultured at  $5 \times 10^3$  cells/well in 96-well cell culture plates, and cultured at 37°C and 5% CO<sub>2</sub>. After 48 hours of culture, the luciferase activity of each cell clone was detected using a ONE-Glo Luciferase Assay System (Promega). Subsequently, the cell clone with the highest fluorescence value was continuously cultured for 6 to 8 weeks, and its luciferase activity (RLU) was detected every 5 generations using the luciferase assay kit to observe whether the luc gene was stably expressed.

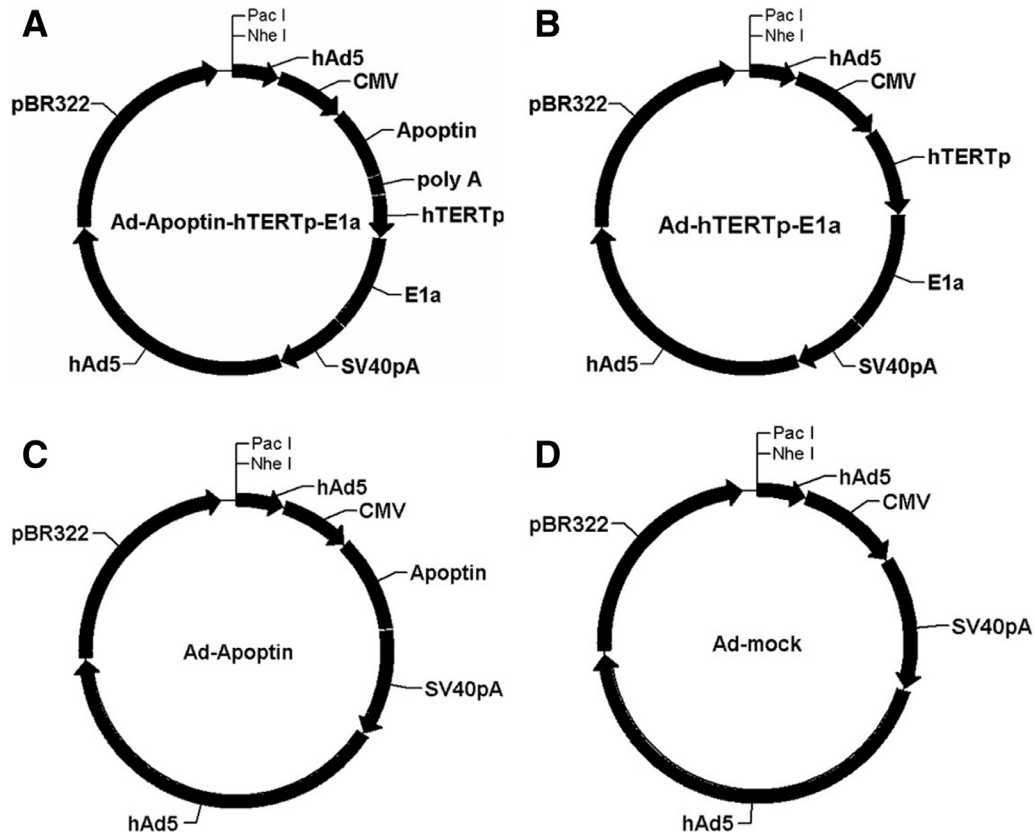


Fig. 1. Schematic diagram of four recombinant adenovirus vectors constructed using shuttle vectors.

(A) Ad-VT. (B) Ad-T. (C) Ad-vp3. (D) Ad-mock.

### 2.3. Detecting the biological characteristics of PC-3-luc cells

The characterization of PC-3-luc cells was performed using cell growth curve, cell cycle assays, and immunoblotting. The PC-3 and PC-3-luc cells were cultured at  $5 \times 10^3$  cells/well in 96-well cell culture plates, and cultured at conditions of 37°C and 5% CO<sub>2</sub> for 24 hours. A 96-well cell culture plate was taken at each of 7 different time points (1, 2, 3, 4, 5, 6, and 7 days), and the culture solution of each well was discarded, and then 110  $\mu$ l WST-1 solution was added to each well (10  $\mu$ l WST-1 and 100  $\mu$ l serum-free and no anti-antibody DMEM medium), cultured continued for 1.5 hours in the dark, and the absorbance at 450 nm was then measured.

The PC-3 and PC-3-luc cells were cultured at  $2 \times 10^5$  cells/well in 12-well cell culture plates, and cultured at 37°C and in 5% CO<sub>2</sub> for 24 hours. The PC-3 and PC-3-luc cells were harvested and washed 3 times with phosphate-buffered saline (PBS). The PC-3 and PC-3-luc cells were resuspended in 5 ml 75% ethanol (precooled at 4°C) and incubated at 4°C for 18 hours in the dark. Subsequently, the PC-3 and PC-3-luc cells were washed 3 times with PBS and then 500  $\mu$ l propidium iodide (PI)/RNase solution was added. After 20 minutes of incubation, the sample was transferred to a labeled flow tube and detected using flow cytometry (BD Bioscience Clontech, San Diego, CA).

The PC-3 and PC-3-luc cells were cultured at  $5 \times 10^5$  cells/well in 6-well cell culture plates, and cultured at 37°C and in 5% CO<sub>2</sub> for 24 hours. The PC-3 and PC-3-luc cells were collected by centrifugation. Cell lysates were used to resuspend the cells, then they were stored on ice bath for 5 minutes. They were centrifuged at 600 g for 5 minutes and the supernatant was centrifuged obtain both the cytosol and the mitochondria. The precipitants were dissolved by buffer (10 mmol/L Tris [pH 7.4], 150 mmol/L NaCl, 1% Triton X-100, 5 mmol/L EDTA [pH 8.0]); all samples were analyzed by Western blotting. The following primary antibodies were used: rabbit  $\beta$ -actin (Cat. 4970), rabbit anti-Cyclin D1 (Cat. 2978), rabbit anti-CDK2 (Cat. 2546) (all from Cell signaling technology, Danvers MA). The following secondary antibodies were used: Peroxidase-Conjugated Goat anti-Rabbit IgG (H+L) (Cat. ZB2301, ZSGB-BIO, CN).

### 2.4. Crystal violet staining assay

Cell survival was measured using crystal violet staining to observe the inhibition of recombinant adenovirus on the growth of the PC-3-luc cells. The PC-3-luc cells were cultured at  $2 \times 10^5$  cells/well in 12-well cell culture plates, and cultured at 37°C and in 5% CO<sub>2</sub> for 24 hours. Subsequently, the PC-3-luc cells were infected with different concentrations of recombinant adenovirus (1 multiplicity of infection [MOI], 10 MOI, and 100 MOI). At 24, 48, 72, and 96 hours, the culture medium in each well was discarded

and the plates were turned over on a filter paper for 1 minute, and then 350  $\mu$ l of 0.1% crystal violet solution were added to each well for the staining at room temperature for 10 minutes. The staining solution was carefully sucked dry by turning the plates over on a filter paper. The inhibitory effects of the recombinant adenovirus on the growth of the PC-3-luc cells were then observed.

### 2.5. MTS assay

PC-3-luc cells were cultured at  $5 \times 10^3$  cells/well in 96-well cell culture plates, and cultured at 37°C and 5% CO<sub>2</sub> for 24 hours. After 24 hours of culture, the cells were infected with different concentrations of recombinant adenovirus (1 MOI, 10 MOI, and 100 MOI), and blank control wells were set. At 24, 48, 72, and 96 hours, 20  $\mu$ l MTS (3-[4,5-dimethylthiazol-2-yl]-5-[3-carboxymethoxyphenyl]-2-[4-sulfophenyl]-2H-tetrazolium) solution (cell proliferation assay reagent; Promega) and 100  $\mu$ l cell culture medium were mixed, and then added to each well, and incubation continued at 37°C and 5% CO<sub>2</sub> for 1 to 2 hours. Subsequently, the absorbance at 490 nm was measured. We calculated the cell viability as follows:  $100 \times (\text{absorbance of virus-treated wells} / \text{absorbance of control wells})$  [30,31].

### 2.6. Hoechst assay

PC-3-luc cells were cultured at  $2 \times 10^5$  cells/well in 12-well cell culture plates, and cultured at 37°C and in 5% CO<sub>2</sub> for 24 hours. Subsequently, the cells were infected with different concentrations of recombinant adenovirus (1 MOI, 10 MOI, and 100 MOI). At 24, 48, 72, and 96 hours, the PC-3-luc cells were harvested and washed 3 times with PBS. PC-3-luc cells were resuspended in 50  $\mu$ l PBS and then 1  $\mu$ l of the Hoechst solution was added. After 15 minutes of incubation, a 10  $\mu$ l sample was applied to a microscope slide with a cover slip, and then observed and photographed under a fluorescence microscope (BX-60, Olympus, Tokyo, Japan). Tests were performed in triplicate and at least 500 cells were scored for each sample to determine the nuclear changes.

### 2.7. Annexin V analysis

PC-3-luc cells were infected with the recombinant adenoviruses (100 MOI). After 48 hours, the cells ( $2 \times 10^5$ ) were harvested and resuspended in binding buffer and stained with fluorescein isothiocyanate (FITC)-labeled Annexin V (Annexin V-FITC Apoptosis Detection Kit; BioVision, Mountain View, CA) according to the manufacturer's protocols. To exclude late apoptotic and necrotic cells, PI was added to the FITC-Annexin V-stained samples. The samples were then examined by flow cytometry (FACSCalibur, Becton Dickinson, Franklin Lakes, NJ) for apoptosis analysis (Cell Quest Pro, Becton Dickinson).

## 2.8. Caspase analysis

The PC-3-luc cells were cultured at  $2 \times 10^5$  cells/well in 12-well cell culture plates, at 37°C and in 5% CO<sub>2</sub> for 24 hours. The cells were infected with 100 MOI recombinant adenovirus for 48 hours. The cells were then harvested and washed 3 times with PBS. PC-3-luc cells were resuspended with lysis buffer before total protein was extracted. The caspase-3, 6, and 7 activities were then analyzed using Caspase Activity Assay Kits (Beyotime Institute of Biotechnology, Shanghai, China). The untreated PC-3-luc cells were set as controls.

## 2.9. JC-1 assay

JC-1 can detect qualitative and quantitative changes in mitochondrial membrane potential (MMP).

PC-3-luc cells were cultured at  $3 \times 10^5$  cells/well in 6-well cell culture plates with a sterile cell slide placed in each well, and cultured at 37°C and 5% CO<sub>2</sub> for 24 hours. Subsequently, the cells were infected with recombinant adenovirus at 100 MOI. A 6-well plate was selected at 3 different time points (24, 48, and 72 hours), the liquid was discarded, 1 ml JC-1 solution was added, and the plate incubated for 15 minutes in the dark. The plates were washed 3 times with PBS and then the cells were observed and photographed using fluorescence microscopy.

PC-3-luc cells were cultured at  $5 \times 10^3$  cells/well in 96-well cell culture plates, and cultured at 37°C and 5% CO<sub>2</sub> for 24 hours. After 24 hours of culture, PC-3-luc cells were infected with recombinant adenovirus at 100 MOI, and blank control wells were set. At 24, 48, and 72 hours, 100 μl of JC-1 solution (Promega) added to each well, incubated at 37°C, 5% CO<sub>2</sub> for 15 minutes in the dark, and then washed 3 times with PBS. Subsequently, the absorbance at 435 nm and 585 nm were measured.

## 2.10. Cell scratch assay

PC-3-luc cells were cultured at  $1 \times 10^6$  cells/well in 6-well cell culture plates, at 37°C and 5% CO<sub>2</sub> for 24 hours. When the cells became more than 90% confluent, the culture medium in each well was discarded. A sterile micropipette tip was then used to make a scratch in the cell layer from one end of the 6-well cell culture plate to the other. The cells were washed with PBS 3 times and images were captured under an inverted microscope (0 hour). Subsequently, the PC-3-luc cells were infected with recombinant adenovirus at 1 and 10 MOI. The 6-well cell culture plates photographed under an inverted microscope at 24 and 48 hours. The width of the scratches at each time point was measured. The experiment was repeated 3 times, and cell migration was calculated according to the following formula: Cell mobility = (0 hour scratch width - 24/48 hours scratch width)/0 hour scratch width.

## 2.11. Transwell invasion and migration assay

PC-3-luc cells were cultured at  $5 \times 10^4$  cells/well in a 24-well cell culture plate at 37°C and 5% CO<sub>2</sub> for 24 hours. The cells were infected with recombinant adenovirus at 10 and 100 MOI for 24 and 48 hours. The cells were then seeded in the upper chamber of the cell culture inserts after trypsinization, and cultured for 24 hours. Cells that had migrated through the membrane were counted under a microscope after they were fixated by carbinol and stained with crystal violet. The experimental procedure of matrigel invasion assay was the same as that for the transwell migration assay except for incubation with matrigel (1:7 with DMEM) in the upper chamber for 1 hour before seeding the cells.

## 2.12. Tumor xenograft experiments

The xenograft models were established via subcutaneous injection of PC-3-luc cells ( $1 \times 10^6/100 \mu\text{l}$ ) into the right legs of mice. When the tumors had formed clearly (usually 7 days), the mice were divided randomly into 5 groups ( $n = 50$ ). Group 1 was injected with  $1 \times 10^8$  plaque forming units (PFU) of Ad-VT in 100 μl of PBS. Group 2 was injected with  $1 \times 10^8$  PFU of Ad-T in 100 μl of PBS. Group 3 was injected with  $1 \times 10^8$  PFU of Ad-vp3 in 100 μl of PBS. Group 4 was injected with  $1 \times 10^8$  PFU of Ad-mock in 100 μl of PBS. Group 5 was injected with 100 μl of PBS. The xenograft models were infected with recombinant adenovirus via intratumoral injection. After successfully establishing xenograft models of nude mice, injections were given twice a week for 3 consecutive weeks. Starting from 0 week, the tumor site of the nude mice was photographed once a week using in vivo living imaging equipment (Merc, Berlin, German), and photographed continuously for 5 weeks. Then, the measurement time (week) was taken as the abscissa and the average bioluminescence value of the tumor (mean photons/s) was taken as the ordinate to plot the average bioluminescence curve of the tumor. The length and width of the xenograft tumors were measured weekly using Vernier calipers from 0 week, and were continuously measured for 5 weeks. The tumor volume was calculated using the following formula:  $0.52 \times (\text{smallest diameter})^2 \times (\text{largest diameter})$ . The percent tumor inhibition was calculated using the formula:  $(1 - \text{treatment group tumor weight/control tumor weight}) \times 100\%$  [30,32,35]. After successfully establishing xenograft models of nude mice, the survival of nude mice was recorded every day, and from 6 weeks was recorded continuously. The survival curve of the nude mice was plotted with survival time (day) as the abscissa and survival rate as the ordinate.

## 2.13. Statistical analysis

Statistical analysis was conducted using data from at least 3 independent experiments. SPSS or SigmaStat 3.5 (Systat Software) was used for the analysis.  $P < 0.05$  was

considered to indicate statistical significance. Data are presented as the mean  $\pm$  standard deviation (SD).

### 3. Results

#### 3.1. Construction and identification of PC-3-luc

The cells were seeded into 96-well plates at  $5 \times 10^3$  cells per well, and after 48 hours, luciferase activities of different clones were determined. The two clones with the highest RLU were Clone 17 and Clone 21 (Fig. 2A); these two clones were retained for luciferase stability assay.

Clone 17 and Clone 21 were amplified and passaged, and the RLU was tested every fifth generation. Clone 17 had the highest RLU when it was passed to the 40th generation, and the RLU measured by this clone in the 40th passage was not significantly different from the initial value ( $P > 0.05$ ) (Fig. 2B), which indicated that Clone 17 could stably express luciferase after 40 passages.

Clone 17 was sequentially diluted and seeded into a 96-well plate at a ratio of 1:2. After the addition of the fluorescein substrate, the bioluminescence intensity and cell number of PC-3-luc presented a certain linear relationship ( $R^2 = 0.9982$ ), and the number of cells that could be detected was less than 100. The luminescence intensity increased with the increase in cell number of cells, further proving that Clone 17 could stably express luciferase (Fig. 2C and D).

#### 3.2. Characterization of PC-3-luc

PC-3 cells and PC-3-luc cells were seeded in 96-well plates, and the OD values of PC-3-luc cells and PC-3 cells were detected by adding WST-1 solution at different time points. As shown in Fig. 2E, the growth trend of PC-3 cells and PC-3-luc cells was similar, and the growth curve was basically consistent, indicating that the construction process had no significant effect on the growth characteristics of the cells ( $P > 0.05$ ) (Fig. 2E).

The collected PC-3-luc cells and PC-3 cells were permeabilized, stained with PI/RNase, and then placed in a flow tube and the cell cycle was detected by flow cytometry. The results showed that both cells were mainly in G1 phase, and the proportion of G2 phase and S phase was also basically the same, with no significant differences in the cell cycle between the 2 cell types ( $P > 0.05$ ) (Fig. 2F and G). Furthermore, we used western blot to detect cell cycle regulators of PC-3 and PC-3-luc cells. The results showed that there was no significant difference in the expression levels of Cyclin D1 and CDK2 in PC-3 and PC-3-luc cells ( $P > 0.05$ ) (Fig. 2H).

#### 3.3. Inhibitory effect of recombinant adenoviruses on the proliferation of human prostate cancer cells

First, we used crystal violet staining to verify whether the recombinant adenoviruses could inhibit PC-3-luc cell

proliferation. Recombinant adenoviruses Ad-VT, Ad-T, Ad-vp3, and Ad-Mock were infected into PC-3-luc cells, separately, and stained with 0.4% crystal violet. As shown in Fig. 3A, recombinant adenoviruses Ad-VT, Ad-T, and Ad-vp3 significantly inhibited cell proliferation relative to Ad-mock, in a dose- and time-dependent manner. The inhibitory effect was strongest in the order Ad-VT > Ad-T > Ad-vp3, indicating that Ad-VT, Ad-T, and Ad-vp3 have a certain killing effect on PC-3-luc cells.

Subsequently, we performed a quantitative experiment on the cell inhibition rate using the MTS assay. PC-3-luc cells were inoculated with recombinant adenoviruses Ad-VT, Ad-T, Ad-vp3, and Ad-Mock, separately, and added to MTS at 24, 48, 72, and 96 hours for detection. As shown in Fig. 3B, at 4 different time points (24, 48, 72, and 96 hours), Ad-VT, Ad-T, and Ad-vp3 inhibited PC-3-luc cell proliferation, while Ad-Mock had no inhibitory effect on the cells; at 1 MOI, the inhibitory effects of Ad-VT, Ad-T, and Ad-vp3 on PC-3-luc cells did not change significantly with increased infection time ( $P > 0.05$ ); at 10 MOI, the inhibitory effect of Ad-VT, Ad-T, and Ad-vp3 on PC-3-luc cells increased with increased infection time, showing a certain time effect ( $P < 0.05$ ). From 48 to 72 hours, the inhibition of PC-3-luc proliferation by Ad-VT fluctuated between 25% and 38%, while the inhibition of Ad-T and Ad-vp3 on PC-3-luc cells was less than 25%. In general, the inhibition of cell proliferation by these 3 recombinant adenoviruses increased with increasing infection time; at 100 MOI, the inhibitory effect of Ad-VT, Ad-T, and Ad-vp3 on cells increased significantly with time, showing an obvious time effect ( $P < 0.05$ ). During infection, the percent inhibition of PC-3-luc proliferation by Ad-VT and Ad-T were the highest (55%–65% and 40%–50%, respectively) at 72 hours, while the inhibition induced by Ad-vp3 was the highest at 96 hours (about 30%). The strongest inhibition was observed in the order: Ad-VT > Ad-T > Ad-vp3 at the 4 different time points (24, 48, 72, and 96 hours). At the same time, the extent of inhibition by Ad-VT, Ad-T and Ad-vp3 increased with increasing infection dose (100 MOI > 10 MOI > 1 MOI), showing a significant dose-effect relationship. The results showed that Ad-VT has a very significant tumor killing effect, and the killing effect has a time- and dose-effect relationship.

#### 3.4. Recombinant adenoviruses induces selective apoptosis of prostate cancer cells

Hoechst is a dye that can enter the cell freely and combine with cell nucleic acid to display blue fluorescence, which effectively shows changes of the nucleus. The staining results at different time points are shown in Fig. 4A. PC-3-luc cells were infected with Ad-VT, Ad-T, Ad-vp3, and Ad-Mock, and the nuclei of PC-3-luc cells infected with Ad-VT, Ad-T, and Ad-vp3 presented different degrees of bright blue hyperchromatism or fragmentation, while the nuclei of Ad-mock group showed uniform blue fluorescence. This

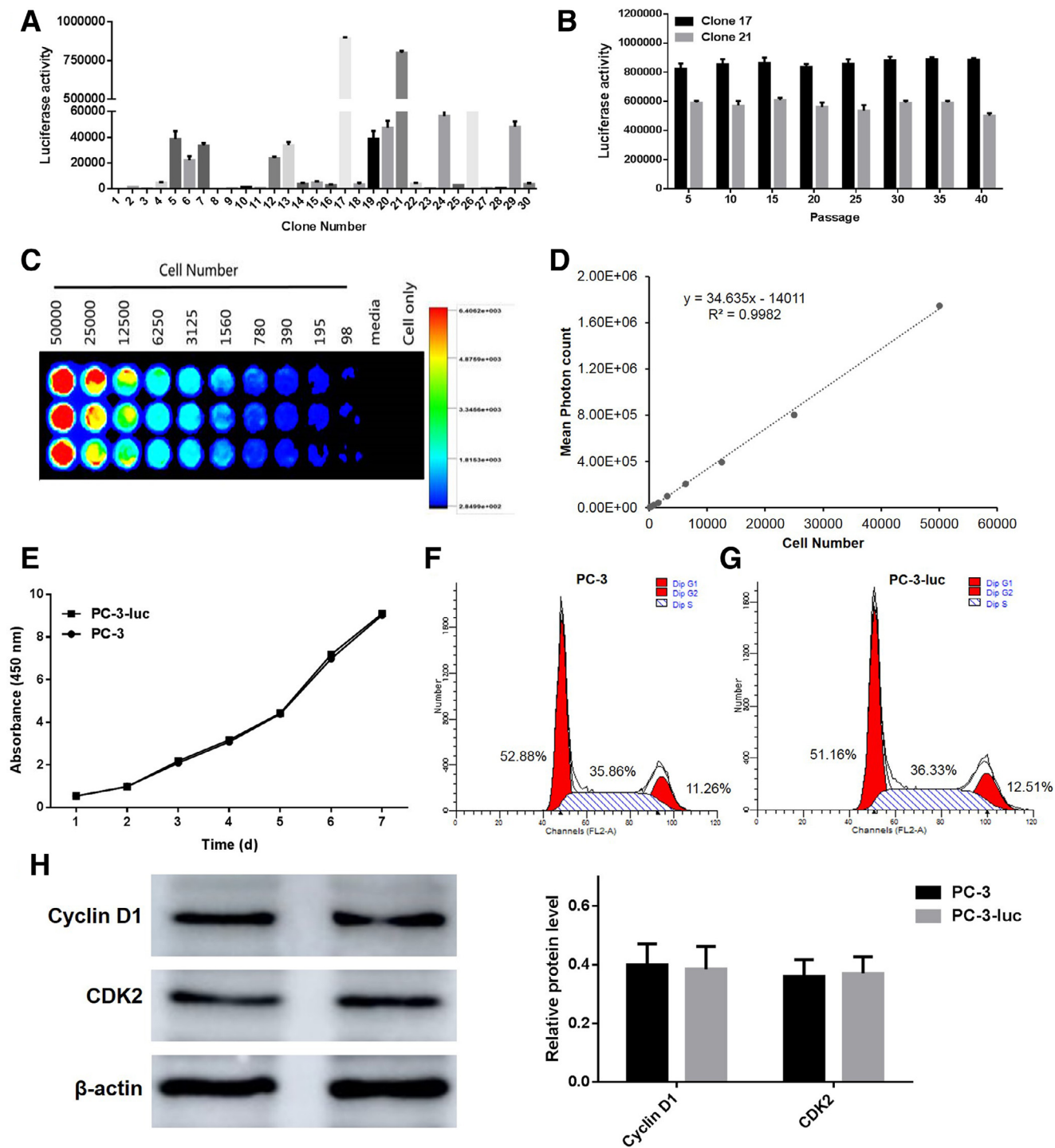


Fig. 2. Screening and identification of PC-3-luc cells.

(A) After transfection of the pGL4.51 plasmid, the two cell clones with the highest luciferase activity were screened with 800  $\mu\text{g}/\text{ml}$  of G418. (B) The luciferase activity of each cell clone was detected using a ONE-Glo<sup>TM</sup> Luciferase Assay System. Subsequently, the luciferase activity (RLU) of cell clones was detected every five generations using the luciferase assay kit to observe whether the luc gene was stably expressed. (C and D) The cell clone with the highest luciferase activity was inoculated in 1:2 ratio into a 96-well plate. After adding fluorescein, the relationship between bioluminescence intensity and cell number was observed. The cell bioluminescence intensity increased with the increase of cell number, and proved that Clone 17 could stably express luciferase. (E) The PC-3 and PC-3-luc cells were cultured in 96-well cell culture plates, and cell growth trends were detected at 1, 2, 3, 4, 5, 6, and 7 days. (F) The PC-3 and PC-3-luc cells were cultured in 12-well cell culture plates, and cell cycles were detected using flow cytometry. (H) Western blotting analysis of PC-3 and PC-3-luc cells extracts for Cyclin D1 and CDK2.

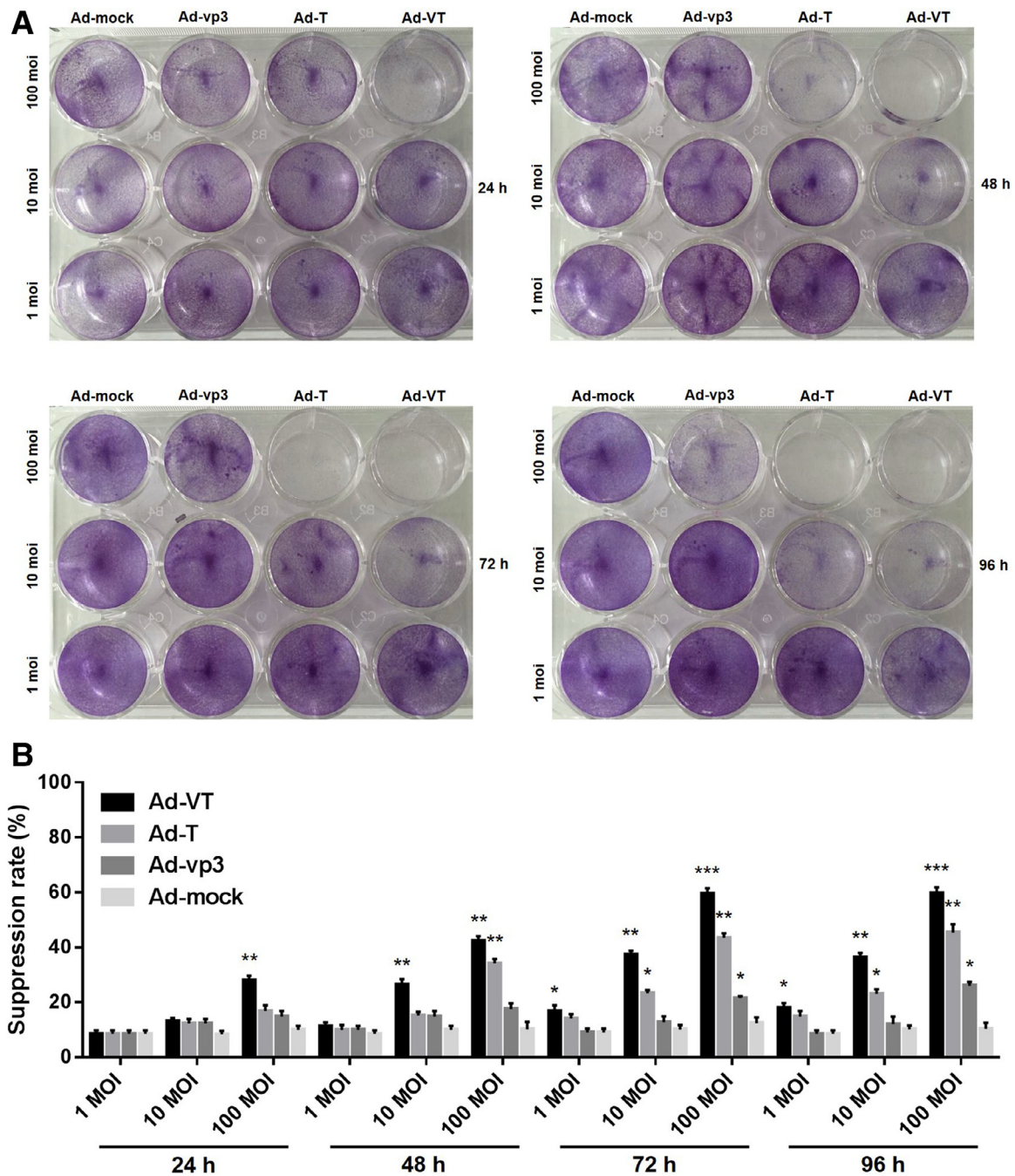


Fig. 3. Effect of the four recombinant adenovirus strains on the cell proliferation in human prostate cells (PC-3-luc).

(A) Confluent monolayers of PC-3-luc cells in 12-well plates were infected with Ad-VT, Ad-T, Ad-vp3, and Ad-mock, and then stained with 0.4% crystal violet at 24, 48, 72, and 96 hours. The Ad-VT, Ad-T, and Ad-vp3 could inhibit PC-3-luc cell proliferation. (B) PC-3-luc cell viability was determined using the MTS assay after Ad-VT, Ad-T, Ad-vp3, and Ad-mock treatment at various concentrations (1, 10, and 100 MOI) for 24, 48, 72, and 96 hours. All measurements were performed in triplicate. Data are presented as the means  $\pm$  standard deviation (SD). In PC-3-luc cells, Ad-VT, Ad-T, and Ad-vp3 infections induced significant growth inhibition. \*  $P < 0.05$ , \*\*  $P < 0.01$ , \*\*\*  $P < 0.001$ , compared with that induced by Ad-mock.

demonstrated that the cells showed certain apoptotic characteristics after infection with recombinant adenovirus. Other strong evidence for the induction of apoptosis by the recombinant adenovirus in PC-3-luc cells was the Annexin V analysis. As shown in Fig. 4B, the 3 recombinant adenoviruses Ad-VT, Ad-T, and Ad-vp3 could induce apoptosis of PC-3-luc at 3 different time points (24, 48, and 72 hours), but the

degree of apoptosis varied. Fig. 4B shows that the apoptosis rates of Ad-VT, Ad-T, and Ad-vp3 at different time points are: Ad-VT > Ad-T > Ad-vp3, in which Ad-VT induced the highest apoptosis rate at all 3 time points; Ad-VT- and Ad-T-induced apoptosis had a significant time effect ( $P < 0.05$ ). The apoptosis rate of Ad-vp3 group was highest at 48 hours and decreased slightly at 72 hours. In summary, the

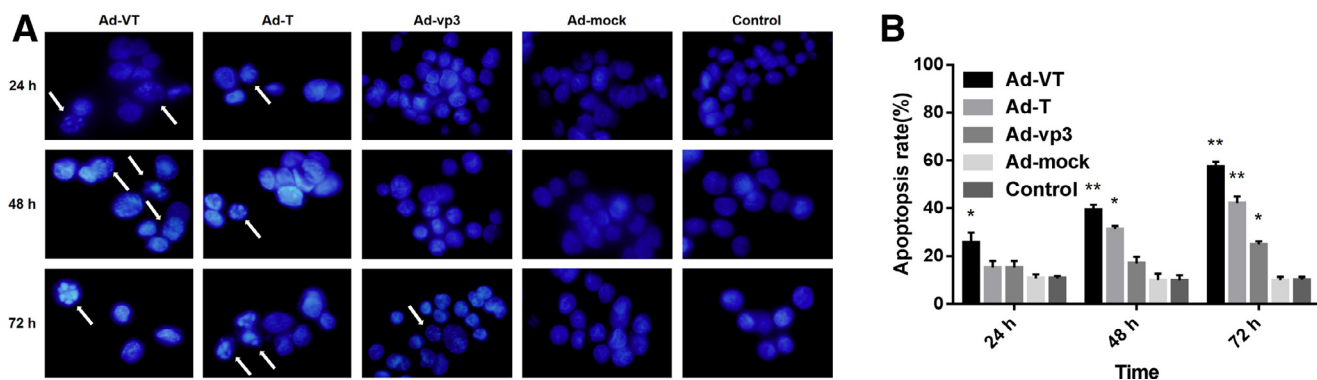


Fig. 4. Identification of PC-3-luc cell apoptosis induced by recombinant adenovirus using Hoechst and Annexin V staining.

(A) Morphological changes under fluorescence microscopy after Hoechst staining. PC-3-luc cells were treated with Ad-VT, Ad-T, Ad-vp3, and Ad-mock for 24, 48, and 72 hours and compared with untreated cells. After the cells were infected with the recombinant adenovirus, in addition to the mock group, the phenomenon of nuclear thickening and nuclear fragmentation increased significantly with the prolongation of time. (B) The PC-3-luc cells were analyzed by flow cytometry after Annexin-V and PI staining. We quantified the percentage of apoptotic cells: The PC-3-luc cells infected with Ad-VT, Ad-T, and Ad-vp3 all showed overt apoptosis. Data are shown as the mean  $\pm$  SD. \*  $P < 0.05$ , \*\*  $P < 0.01$ , compared with the control.

recombinant adenovirus Ad-VT induced apoptosis in PC-3-luc cells specifically.

### 3.5. Recombinant adenovirus induces apoptosis through the mitochondrial pathway

The activation of caspases was then determined (Fig. 5C). Infection of PC-3-luc cells with Ad-VT, Ad-T, and Ad-vp3 caused a marked increase in the levels of caspases-3, 6, and 7. We also evaluated the effects of recombinant adenoviruses on the MMP. The 4 recombinant adenoviruses, Ad-VT, Ad-T, Ad-vp3, and Ad-Mock, were inoculated into PC-3-luc cells, respectively, and stained with JC-1 at 24, 48, and 72 hours, respectively.

As shown in Fig. 5A and B, compared with the ad-mock, the inhibitory effect of Ad-VT, Ad-T, and Ad-vp3 on PC-3-luc cells was demonstrated by changes in the MMP at different time points. The different recombinant adenoviruses have varying abilities to induce apoptosis, as reflected in the different degrees of MMP depolarization. The ability of Ad-VT and Ad-T to induce apoptosis increased with time. The apoptotic cells gradually increased, and the JC-1 gradually changed from the initial red aggregate to the green monomer. By 72 hours, the number of apoptotic cells was the largest, and the ratio of red fluorescence to green fluorescence was the most significant ( $P < 0.05$ ). However, the ability of Ad-vp3 to induce apoptosis did not change significantly with increased time. At 48 hours, the number of apoptotic cells was the largest, that is, the ratio of red fluorescence to green fluorescence decreased, but at 72 hours, the ratio of red fluorescence to green fluorescence increased slightly. At all 3 different time points, the ratio of red fluorescence to green fluorescence is: Ad-VT  $<$  Ad-T  $<$  Ad-vp3  $<$  Ad-Mock. Ad-VT had the strongest ability to induce apoptosis through MMP changes, with the highest number of apoptotic cells and the most significant decrease in the red/green fluorescence ratio.

### 3.6. Recombinant adenovirus inhibits migration and invasion of prostate cancer cells

After the scratches were formed, photographs were taken at different time points (0, 24, and 48 hours) (at the same position), and the width of the scratch was calculated. The cell mobility was reflected by the change in the scratch width. The changes were studied to investigate the effect of the 4 recombinant adenoviruses on the migration of PC-3-luc cells. As shown in Fig. 6A-C, the migration of cells infected with Ad-VT and Ad-T was significantly lower than that of cells infected with Ad-vp3 and Ad-Mock; Ad-VT induced the strongest inhibition of cell migration, and at 48 hours, the migration of PC-3-luc cells was 12.11%, which was significantly lower ( $P < 0.05$ ) than that of Ad-Mock group and the control group. Inhibition of migration was strongest in the order: Ad-VT  $>$  Ad-T  $>$  Ad-vp3  $>$  Ad-Mock. The cell scratch assay demonstrated that the migration ability of PC-3-luc cells was inhibited after infection with recombinant adenovirus. In the transwell migration assay, PC-3-luc cells were treated with 4 recombinant adenoviruses for 24 hours and 48 hours, respectively, and then transferred into the chamber. At each time point, we stained the chamber with crystal violet, observed the cell adherence on the bottom wall of the chamber, and calculated the number of cells. As shown in Fig. 7A-C, Ad-VT, Ad-T, and Ad-vp3, but not Ad-Mock, could inhibit the migration ability of PC-3-luc cells, and the extent of inhibition was different. At 24 hours or 48 hours after infection, the inhibitory effect of Ad-VT and Ad-T on cell migration ability showed a significant dose effect ( $P < 0.05$ ), and the inhibition of migration was strongest in the order: Ad-VT  $>$  Ad-T  $>$  Ad-vp3  $>$  Ad-Mock. At 100 MOI and 10 MOI, cells infected with Ad-VT, Ad-T, and Ad-vp3 showed a lower cell migration rate at 48 hours than at 24 hours, indicating a time effect relationship. Similar results were also observed in the Transwell invasion assay (Fig. 8A-C).

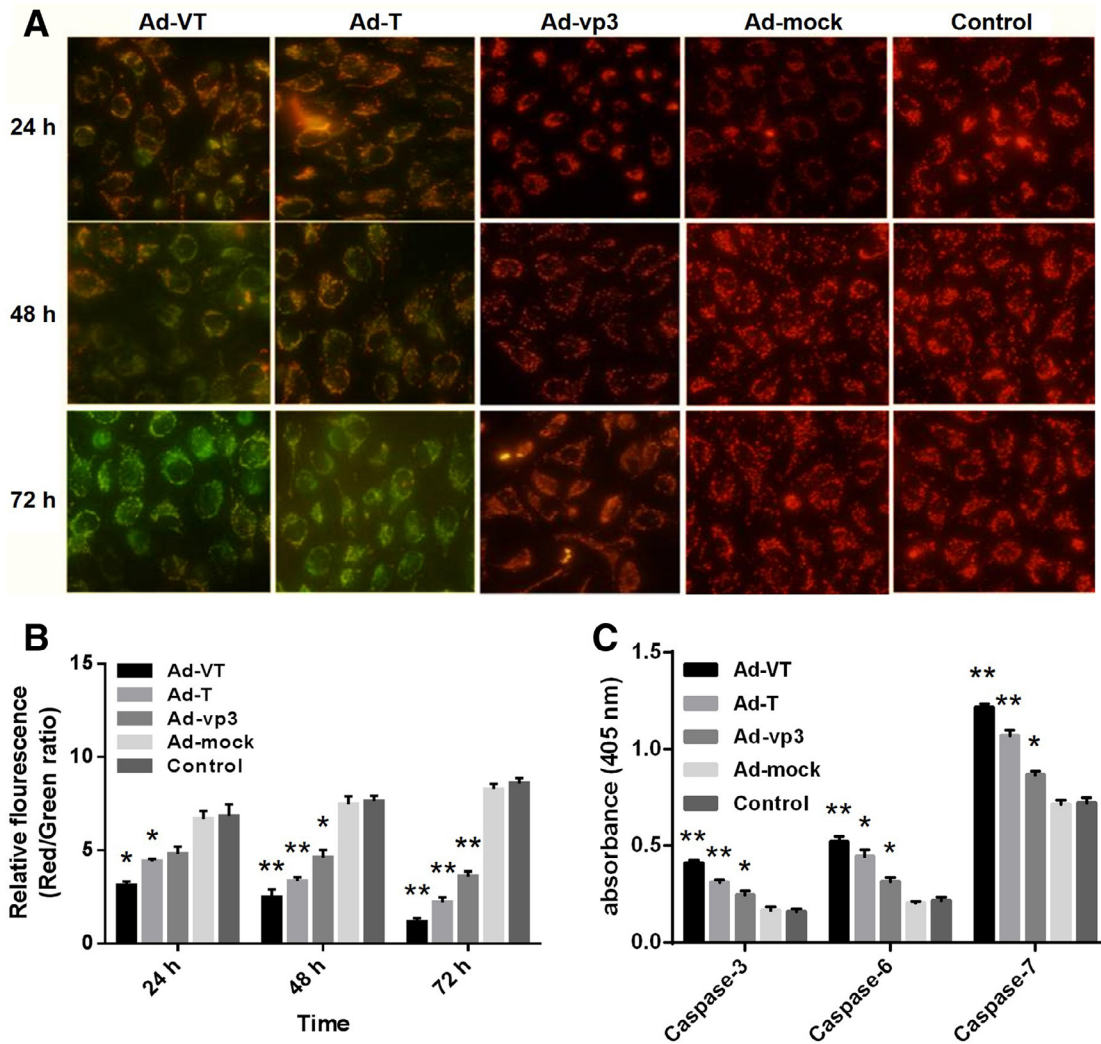


Fig. 5. Analysis of mitochondrial membrane potential of recombinant adenovirus-treated PC-3-luc cells by JC-1 staining and analysis of caspase activation in PC-3-luc cells treated with the recombinant adenoviruses.

(A) Changes in red and green cells under fluorescence microscopy after JC-1 staining. Increased apoptosis results in a decreased ratio of red fluorescence/green fluorescence. (B) We analyzed the change in the ratio of red to green after JC-1 staining quantitatively. Ad-VT, Ad-T, and Ad-vp3 can cause changes in the mitochondrial membrane potential, and Ad-VT had the strongest ability to induce apoptosis by affecting the mitochondrial membrane potential. (C) Cells were treated with the four kinds of recombinant adenoviruses for 48 hours at an MOI of 100. The vertical coordinate for the content of caspases was in units of  $\mu\text{g}/\mu\text{l}$ . Data are the mean  $\pm$  SD. \*  $P < 0.05$ , \*\*  $P < 0.01$ , compared with the control.

The invasion result demonstrated that Ad-VT had strongest ability to inhibit PC-3-luc cells invasion. These results indicated that Ad-VT could significantly inhibit the migration and invasion of PC-3-luc cells in a short period of time.

### 3.7. Antitumor effect of recombinant adenovirus in vivo

We examined the antitumor potential of recombinant adenovirus in a PC-3-luc tumor model.

From the week 0 after the injection of the viruses, the change in the bioluminescence intensity of the tumor was observed using a living body imaging system, and was continuously observed for 5 weeks. The results are shown in Fig. 9A and B. At 0 to 2 weeks, there was no significant difference in the average bioluminescence intensity of the

tumors in each treatment group ( $P > 0.05$ ); at 2 to 3 weeks, the average bioluminescence intensity of the tumors in the Ad-VT treatment group, the Ad-T treatment group, and the Ad-vp3 treatment group increased slightly, but with no significant difference ( $P > 0.05$ ), while the average bioluminescence intensity of the Ad-Mock treatment group and the control group increased rapidly. At 3 to 5 weeks, the average bioluminescence intensity of the Ad-VT treatment group was always lower than that of the other treatment groups; at 4 to 5 weeks, the average bioluminescence intensity of the Ad-VT and Ad-T treatment groups was significantly lower than that of Ad-Mock treatment group and the control group ( $P < 0.05$ ).

After subcutaneous tumor formation, the tumor size was measured continuously for 5 weeks. The results are shown

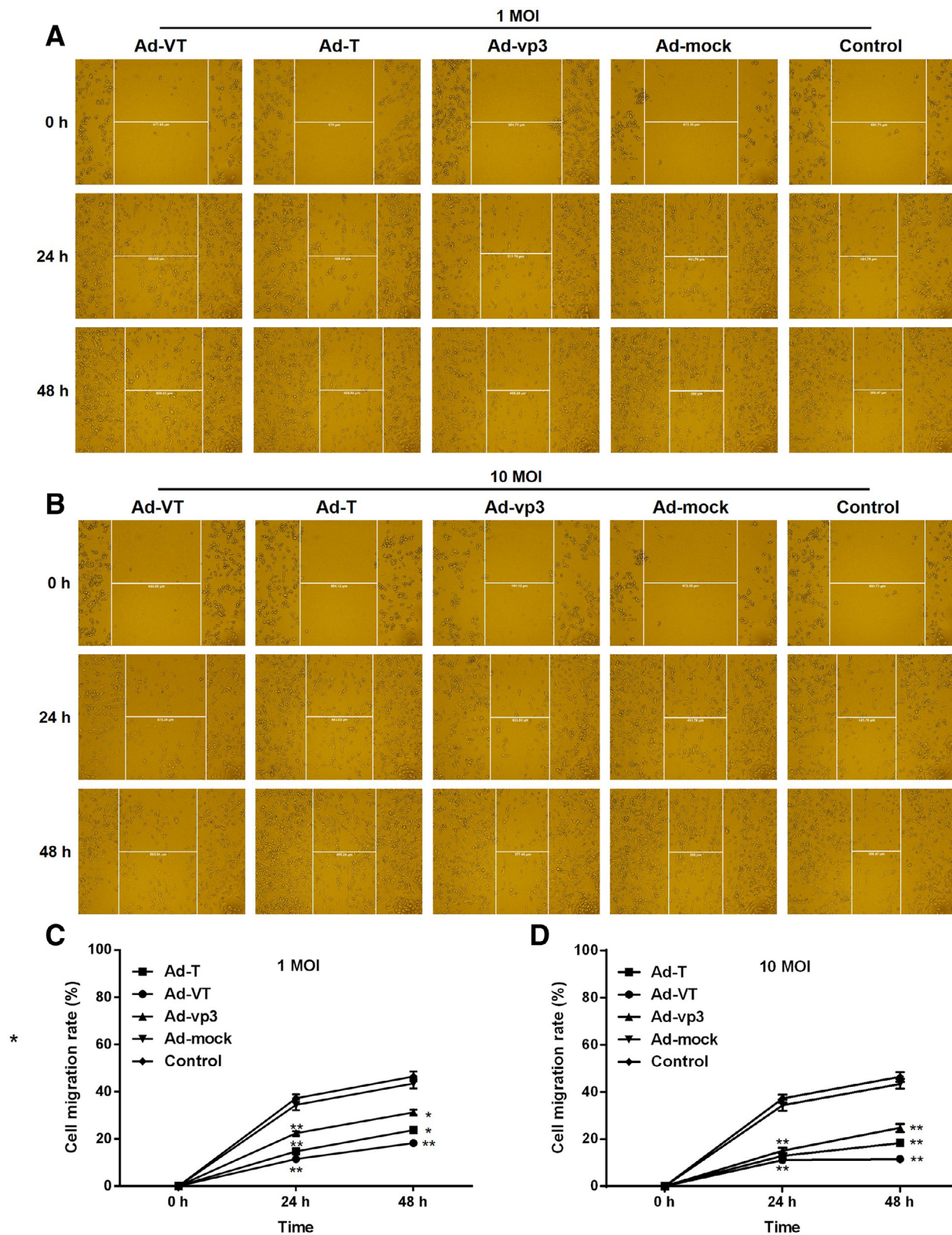


Fig. 6. Identification of PC-3-luc cell mobility induced by recombinant adenovirus with cell scratch assay.

(A and B) The PC-3-luc cells were infected with recombinant adenovirus at 1 and 10 MOI. The width of the scratches in the cell layer at each time point was measured. All measurements were performed in triplicate. (C and D) The cell migration rate was calculated according to the following formula: Cell mobility = (0 hour scratch width – 24/48 hours scratch width)/0 hour scratch width. Data are presented as the means ± standard deviation (SD). \*  $P < 0.05$ , \*\*  $P < 0.01$ , compared with the control.

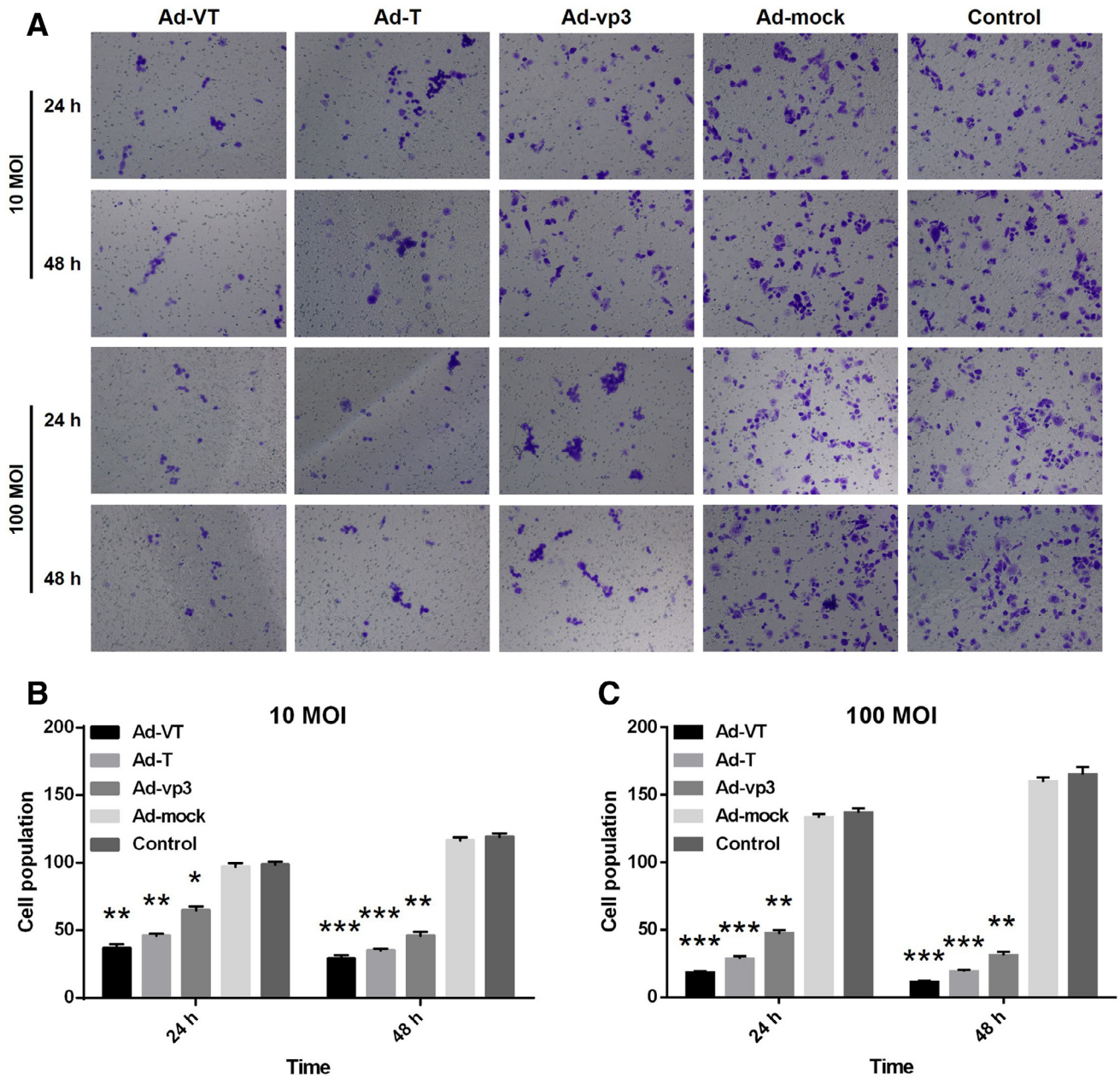


Fig. 7. Migration suppression effects on PC-3-luc cells assessed using the Transwell assay.

(A) The migration suppression of PC-3-luc cells infected with 10 and 100 MOI recombinant adenovirus at 24 and 48 hours. (B and C) Cells that had migrated through the membrane were counted under a microscope after they were fixated with carbinol and stained with crystal violet. Cells infected with Ad-VT showed the lowest migration at 24 and 48 hours. Data are presented as the means  $\pm$  standard deviation (SD). \*  $P < 0.05$ , \*\*  $P < 0.01$ , \*\*\*  $P < 0.001$ , compared with the control.

in Fig. 9C and D. The average tumor growth rate between the control group and the Ad-Mock treatment group was not significantly different ( $P > 0.05$ ); the tumor growth rate of the Ad-T treatment group and Ad-vp3 treatment group became slower at 3 to 4 weeks, and had no significant difference ( $P > 0.05$ ). After 4 weeks, the average growth rate of the tumor in the Ad-T treatment group was slower; however, the average growth rate of tumors in the Ad-vp3 treatment group did not slow down, and was always larger than that in the Ad-T treatment group. Compared with the

Ad-Mock treatment group and the control group, the average growth rate of the Ad-VT treatment group was significantly lower at 4 to 5 weeks ( $P < 0.05$ ). The average growth rate of the Ad-VT treatment group was always lower than that of the other groups at 3 to 5 weeks, indicating that Ad-VT could effectively inhibit the growth of PC-3-luc tumors.

From the tumor growth inhibition curve, it can be seen that the average tumor inhibition rate of the control group, Ad-Mock treatment group, and Ad-vp3 treatment group

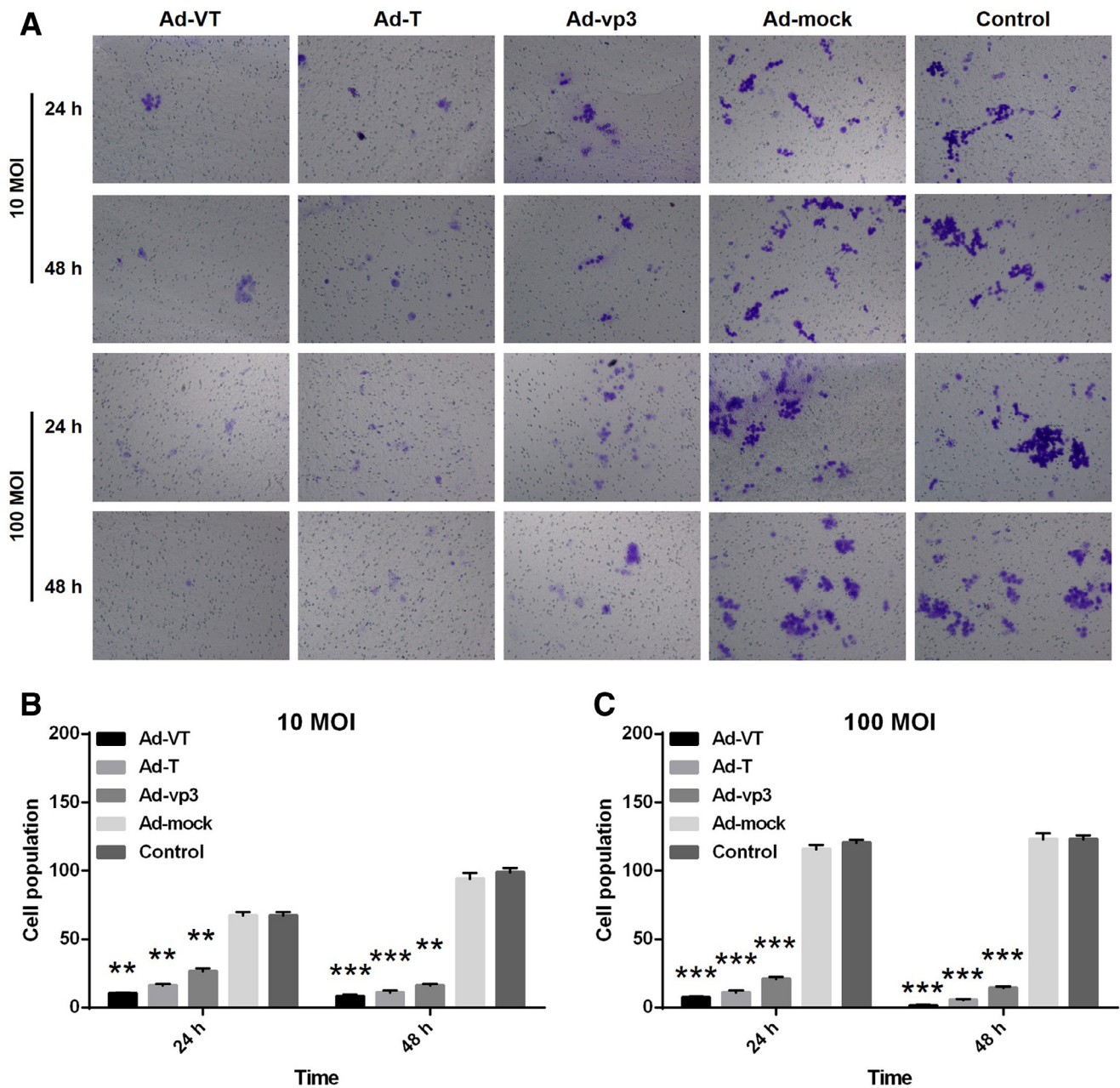


Fig. 8. Invasion suppression effects on PC-3-luc cells assessed using the Transwell assay.

(A) The invasion suppression of PC-3-luc cells infected with 10 and 100 MOI recombinant adenovirus at 24 and 48 hours. (B and C) Cells that had passed through the membrane were counted under a microscope after they were fixated with carbinol and stained with crystal violet. Cells infected with Ad-VT showed the lowest invasion at 24 and 48 hours. Data are presented as the means  $\pm$  standard deviation (SD). \*  $P < 0.05$ , \*\*  $P < 0.01$ , \*\*\*  $P < 0.001$ , compared with the control.

showed no significant change at 0 to 5 weeks ( $P > 0.05$ ); at 2 to 5 weeks, the average tumor inhibition rate of the Ad-VT treatment group was always higher than that of the other groups; the average tumor inhibition rate of the Ad-VT treatment group was significantly higher than that of the Ad-Mock treatment group and the control group at 3 to 5 weeks ( $P < 0.05$ ); and at 5 weeks, the average tumor inhibition rate of the Ad-VT treatment group was as high as 66%, indicating that Ad-VT has a significant tumor inhibition effect.

After inducing subcutaneous tumors, the survival of each group of nude mice was continuously recorded. As shown in Fig. 9E, compared with the other 3 treatment groups (Ad-VT, Ad-T, and Ad-vp3), the mice of the control group and the Ad-mock treatment group began to die from about 23 days after the formation of the subcutaneous tumors, and their average survival times were about 30.8 days and 31.2 days, respectively, with no significant difference ( $P > 0.05$ ). Compared with the Ad-vp3 treatment group, the Ad-Mock treatment group, and the control

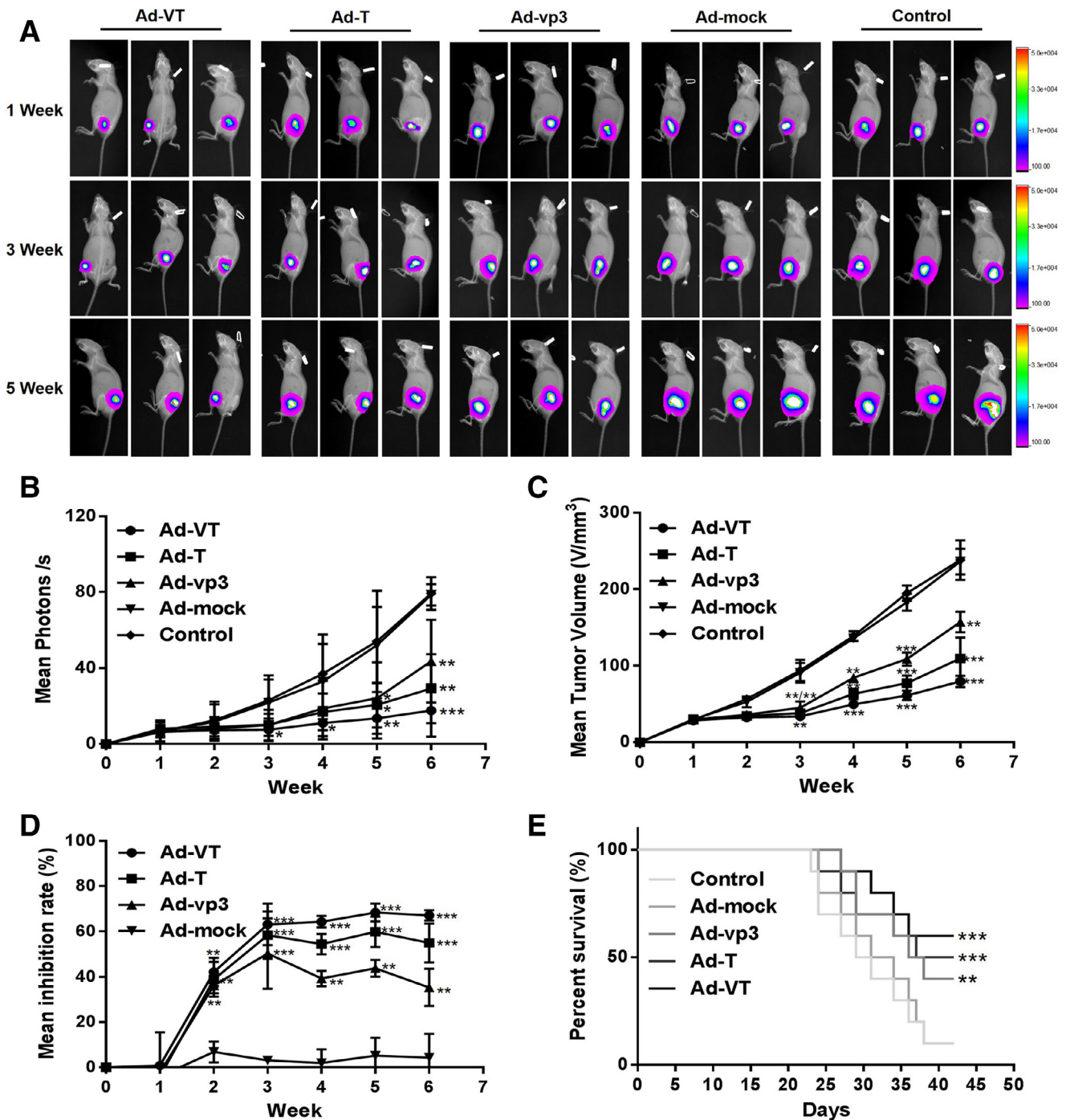


Fig. 9. Effect of recombinant adenovirus on prostate cancer in a BALB/c nude mice model.

(A and B) The xenograft models were established via subcutaneous injection of PC-3-luc cells ( $1 \times 10^6/100 \mu\text{l}$ ) into the right legs of the mice ( $n = 10$  per group). Beginning after tumor formation, *in vivo* bioluminescent imaging was used to continuously monitor changes in tumor bioluminescence intensity. (C and D) The length and width of the xenograft tumors were measured weekly using Vernier calipers from 0 week, and continuously measured to 5 weeks. The % tumor inhibition was calculated using the formula:  $(1 - \text{treatment group tumor weight}/\text{control tumor weight}) \times 100\%$ . (E) After successfully establishing xenograft models in nude mice, the survival of the mice was recorded every day, and 6 weeks was recorded continuously. The average % tumor inhibition of the Ad-VT group was significantly higher than that of the other groups, reaching 66%. Similarly, the survival rate of the Ad-VT group was also the highest, reaching 66.67%. Data are presented as the means  $\pm$  standard deviation (SD). \*  $P < 0.05$ , \*\*  $P < 0.01$ , \*\*\*  $P < 0.001$ , compared with the control (Fig. 9D, compared with the Ad-mock).

group, the average survival time of the Ad-VT and Ad-T treatment groups was about 38 days and 36.1 days, respectively, that is, the survival time was significantly prolonged ( $P < 0.05$ ). The survival time of the Ad-VT treated group

was longer than that of the Ad-T treated group, and at 42 days, the survival rate of the Ad-VT treated mice was 66.67%. This indicates that Ad-VT can increase the survival rate of mice and significantly prolong their survival.

#### 4. Discussion

Cancer is one of the leading causes of death in developed and developing countries [36]. Prostate cancer is the most common cancer among men. The genetic and epigenetic instability of tumor cell is potential driver for malignant progression, which includes evasion of growth inhibition signals, sustainment of replication, inhibition of cell death, stimulation of angiogenesis, cell migration and invasion, reprogramming of energy metabolism and avoidance of immune cells, which are known as "Hallmarks of Cancer" [37,38]. Currently, many researches are focusing on oncolytic virus as a gene therapy for treatment of cancer, however, the main challenge is to monitor and track the effects of gene therapy [39]. With the introduction of molecular imaging technology, these challenges can be overcome. Molecular imaging technology has many advantages which enable to monitor various physiological and pathological changes in a noninvasive and real-time approach.

BLI is based on luciferase-labeled cells or DNA. In the presence of  $O_2$ ,  $Mg^{2+}$ , and adenosine triphosphate, the expression product can catalyze the oxidation of fluorescein and release photons, which is a self-luminescence phenomenon. It does not require excitation light, has high sensitivity, and a low signal-to-noise ratio. It is used to detect subtle changes of deep tissue in a holistic and noninvasive manner, and can quantify the bioluminescence intensity and its correlation with cell number or tumor volume can be analyzed [40–42]. The most widely used is firefly luciferase, whose main advantages are: A very low level of luciferase can be detected with a simple instrument with high sensitivity; light emission can be detected in cuvettes, microplates, and petri dishes, and can be tested *in vivo*; and adenosine triphosphate is the energy currency of all living cells [43,44]. In the present study, the plasmid pGL4.51 was used to transfect cells to construct tumor cells that stably expressed luciferase (PC-3-luc).

In this study, the relationship between the luminescence intensity of PC-3-luc cells and the number of cells was analyzed using *in vitro* imaging experiments, which indicated that there is a linear relationship between the luminescence intensity and the number of cells, for which the correlation coefficient was  $R^2 = 0.9982$ . Cell luminescence increased with the increase in cell number, indicating that the bioluminescence intensity in region of interest could reflect the number of cells in this region, and there was a positive correlation between the cell number and bioluminescence intensity, providing a cytological basis for establishing a tumor model that could be observed by the living imaging system. Subsequently, the biological characteristics of PC-3-luc cells and PC-3 cells were compared. The results showed that PC-3-luc cells and PC-3 cells have similar growth trends and cell cycles. In mice, PC-3-luc cells could be used to replace PC-3 cells to establish a tumor model, and the tumor growth and metastasis, and the antitumor drug effect, were studied through the living imaging system.

Viral protein 3 (VP3) from CAV, which induces apoptosis in chick thymocytes, was named as "Apoptin" because it can induce apoptosis of various cells [21,45,46]. Apoptin selectively induces apoptosis in a variety of cancer cells, but has no effect on normal cells [30,47–51]. Studies have shown that apoptin has different nuclear localizations in tumor cells and normal cells, explaining its ability to selectively kill tumor cells. Mutating the nuclear localization signal of apoptin suggested that its nuclear localization is closely related to the induction of tumor cell apoptosis [52]. Studies have also shown that apoptin in cells has a tropism, transporting from high to low concentrations, and the ability to induce apoptosis is dose-related [53]. Other studies have shown that apoptin mainly accumulates in the nuclei of tumor cells and causes cell death, including in cells with a P53 mutation or Bcl-2 overexpression [54].

Telomerase is responsible for the extension of the ends of chromosomes in DNA synthesis, which occurs in germ cells as well as in most malignant cells. The constitutive expression of hTR and hTERT of the telomerase is mainly dependent on the transcription of *hTERT*. In the former, the expression is abnormal and the activity is high, while in the latter, it is almost not expressed and the activity is low. In most cancers, up-regulation of *TERT* mRNA expression and down-regulation of tumor suppressor genes, such as Rb and p16, may maintain the immortalization of cancer cells [54]. Human hTERT act as tumor specific promoter for oncolytic adenoviruses. hTERT promoter fragment, which in the context of replication-conditional adenovirus Ado-hTERT-E1A recapitulated high telomerase promoter-based E1A expression and viral activity in cancer cells [55].

In this study, the inhibitory effect of recombinant adenoviruses on PC-3-luc cells was investigated by crystal violet staining and MTS assays. The results showed that Ad-VT, Ad-T, and Ad-vp3 all had different degrees of inhibitory effect on PC-3-luc cells, with the order of strength and weakness as Ad-VT > Ad-T > Ad-vp3, and had a certain time and dose effect; the inhibition induced by Ad-vp3 was the highest at 96 hours and reached 30%, and it is significantly higher than the Ad-mock. On the other hand, at 100 MOI, the inhibition rate of Ad-VT on PC-3-luc cells was the highest at 72 hours and reached 62.74%, while that of Ad-T was the highest at 72 hours (47.77%). From the above results, we could see that the expression of apoptin protein played a very significant role in the inhibition effect of recombinant adenoviruses on PC-3-luc cells; although Ad-vp3 did not have the ability to replicate in tumor cells, but it expressed apoptin protein; the inhibition effect of Ad-vp3 was significantly higher than that of Ad-mock on PC-3-luc cells. While both Ad-VT and Ad-T contained the *hTERT* promoter, and therefore both had the ability to replicate in tumor cells. It was found that the inhibitory effect of Ad-VT was significantly higher than that of Ad-T on PC-3-luc cells, possibly because Ad-VT has the ability to continuously express apoptin.

Subsequently, the inhibition pathway of recombinant adenovirus on PC-3-luc cells was analyzed using JC-1

staining, Hoechst staining, and Annexin V-FITC/PI flow assay. The results showed that Ad-VT, Ad-T, and Ad-vp3 could induce apoptosis to produce cytotoxicity. The Annexin V flow cytometry results showed that at 100 MOI and 72 hours, the apoptosis rate of Ad-VT group was 58.48%, and the apoptosis rate of Ad-T group was 44.13%, which was consistent with MTS results, further demonstrating that Ad-VT, Ad-T, and Ad-vp3 exert their inhibitory effects mainly by inducing apoptosis. The effects of the recombinant adenoviruses on the migration and invasion of PC-3-luc cells were investigated using a scratch assay, Transwell migration, and invasion assay. The results showed that Ad-VT, Ad-T, and Ad-vp3 could decrease cell migration, invasion, and inhibition in the order Ad-VT > Ad-T > Ad-vp3, and the main reason was that Ad-VT, Ad-T, and Ad-vp3 could kill the cells or decreased the activity of some proteolytic enzymes, which could weaken cell migration and invasion. The specific mechanisms by which the adenoviruses affect cell migration and invasion require further research. In conclusion, Ad-VT, mainly by inducing apoptosis, inhibited the growth, migration, and invasion of PC-3-luc cells, to a greater extent than Ad-T and Ad-vp3, which is related to its specific replication and specific killing ability. Ad-vp3 cannot specifically replicate in PC-3-luc cells, therefore, it can only produce a certain inhibitory effect over a short period.

In this study, a subcutaneous tumor-bearing model of nude mice labeled with luciferase was successfully established. The *in vivo* inhibitory effect of recombinant adenovirus on PC-3-luc-induced tumors was investigated using a living imaging system. The results of *in vivo* imaging in nude mice showed that the average bioluminescence intensity of the tumors in the Ad-VT treatment group was always lower than that in the other groups at 2 to 5 weeks. The average tumor growth curve and the average tumor inhibition curve showed that Ad-VT had a significant antitumor effect, with the inhibition rate reaching 66% at 5 weeks. The survival curve of nude mice showed that the Ad-VT treatment group could significantly prolong the survival of mice: The survival rate was 66.67% at 6 weeks. These results showed that Ad-VT has antitumor effect and significantly prolongs mouse survival.

In short, through a series of *in vitro* and *in vivo* experiments demonstrated that Ad-VT has a significant inhibitory effect on the prostate cancer cell line PC-3.

## 5. Conclusions

In this study, we constructed the human prostate cancer PC-3-luc cells with a stable expression of the luciferase gene and it was have the same biological characteristics as PC-3 cells, so PC-3-luc cells can replace PC-3 cells for *in vivo* and *in vitro* experiments. Ad-VT has the characteristics of tumor-specific replication and specific tumor killing, and through a variety of *in vitro* and *in vivo* experiments, it was confirmed that Ad-VT has a significant inhibitory

effect on PC-3 cells, indicating that Ad-VT has potential clinical development value to treat prostate cancer.

## Author contributions

Ningyi Jin and Xiao Li coordinated the study and provided funding. Weihua Wang coordinated the study too. Chuanxin Cui designed and performed the experiments and analyzed the data. Yujia Sun, Yilong Zhu, Jinbo Fang, Bing Bai, Wenjie Li, Shanzhi Li and Yizhen Ma assisting performed the experiment, Chuanxin Cui wrote the manuscript with substantial contribution, Yiquan Li participated in editing the manuscript. All authors reviewed the results and approved the final version of the manuscript.

## Conflicts of interest statement

The research was conducted in the absence of any commercial or financial relationships that could be construed as a potential conflict of interest.

## Informed consent

Informed consent was obtained from all individual participants included in the study.

## Ethical approval

All applicable international, national, and/or institutional guidelines for the care and use of animals were followed.

## Acknowledgments

This work was supported by the National Key Research and Development Program of China [grant number 2016YFC1200900], the National Science and Technology Major Project (Major New Drugs Innovation and Development) [grant number 2018ZX09301053-004-001], Key Technologies R&D Program of Jilin Province [20160209015YY], and the Major Technological Program of Changchun City [grant number 16ss11].

## References

- [1] Kovac JR, Pan MM, Lipschultz LI, Lamb DJ. Current state of practice regarding testosterone supplementation therapy in men with prostate cancer. *Steroids* 2014;89:27–32.
- [2] Bray F, Sankila R, Ferlay J, Parkin DM. Estimates of cancer incidence and mortality in Europe in 1995. *Eur J Cancer* 2002;38:99–166.
- [3] Jemal A, Siegel R, Ward E, Hao Y, Xu J, Thun MJ. Cancer statistics, 2009. *CA Cancer J Clin* 2009;59:225–49.
- [4] Mathijssen RH, Loos WJ, Verweij J, Sparreboom A. Pharmacology of topoisomerase I inhibitors irinotecan (CPT-11) and topotecan. *Curr Cancer Drug Targets* 2002;2:103–23.
- [5] Siegel RL, Miller KD, Jemal A. Cancer Statistics, 2017. *CA Cancer J Clin* 2017;67:7–30.

- [6] Gokce MI, Wang X, Frost J, Roberson P, Volk RJ, Brooks D, et al. Informed decision making before prostate-specific antigen screening: initial results using the American Cancer Society (ACS) Decision Aid (DA) among medically underserved men. *Cancer* 2017;123:583–91.
- [7] Chen W. Cancer statistics: updated cancer burden in China. *Chin J Cancer Res* 2015;27:1.
- [8] Bell JC, McFadden G. Editorial overview: oncolytic viruses—replicating virus therapeutics for the treatment of cancer. *Curr Opin Virol* 2015;13:viii–ix.
- [9] Russell SJ, Peng KW. Viruses as anticancer drugs. *Trends Pharmacol Sci* 2007;28:326–33.
- [10] Russell SJ, Peng KW, Bell JC. Oncolytic virotherapy. *Nat Biotechnol* 2012;30:658–70.
- [11] Fass L. Imaging and cancer: a review. *Mol Oncol* 2008;2:115–52.
- [12] Brindle K. New approaches for imaging tumour responses to treatment. *Nat Rev Cancer* 2008;8:94–107.
- [13] Deng WP, Yang WK, Lai WF, Liu RS, Hwang JJ, Yang DM, et al. Non-invasive in vivo imaging with radiolabelled FIAU for monitoring cancer gene therapy using herpes simplex virus type 1 thymidine kinase and ganciclovir. *Eur J Nucl Med Mol Imaging* 2004;31:99–109.
- [14] Shah K, Jacobs A, Breakefield XO, Weissleder R. Molecular imaging of gene therapy for cancer. *Gene Ther* 2004;11:1175–87.
- [15] Xu T, Close D, Handagama W, Marr E, Saylor G, Ripp S. The expanding toolbox of in vivo bioluminescent imaging. *Front Oncol* 2016;6:150.
- [16] Zhao H, Doyle TC, Coquoz O, Kalish F, Rice BW, Contag CH. Emission spectra of bioluminescent reporters and interaction with mammalian tissue determine the sensitivity of detection in vivo. *J Biomed Opt* 2005;10:41210.
- [17] Fraga H, Fernandes D, Novotny J, Fontes R, Esteves da Silva JC. Firefly luciferase produces hydrogen peroxide as a coproduct in dehydrolyciferyl adenylate formation. *Chembiochem* 2006;7:92935.
- [18] Kim JB, Urban K, Cochran E, Lee S, Ang A, Rice B, et al. Non-invasive detection of a small number of bioluminescent cancer cells in vivo. *PLoS One* 2010;5:e9364.
- [19] Noteborn MH, de Boer GF, van Roozelaar DJ, Karreman C, Kranenburg O, Vos JG, et al. Characterization of cloned chicken anemia virus DNA that contains all elements for the infectious replication cycle. *J Virol* 1991;65:3131–9.
- [20] Noteborn MH, Koch G. Chicken anaemia virus infection: molecular basis of pathogenicity. *Avian Pathol* 1995;24:11–31.
- [21] Noteborn MH, Todd D, Verschuere CA, de Gouw HW, Curran WL, Veldkamp S, et al. A single chicken anemia virus protein induces apoptosis. *J Virol* 1994;68:346–51.
- [22] Danen-Van Oorschot AA, Fischer DF, Grimbergen JM, Klein B, Zhuang S, Falkenburg JH, et al. Apoptin induces apoptosis in human transformed and malignant cells but not in normal cells. *Proc Natl Acad Sci U S A* 1997;94:5843–57.
- [23] Guelen L, Paterson H, Gaken J, Meyers M, Farzaneh F, Tavassoli M. TAT-apoptin is efficiently delivered and induces apoptosis in cancer cells. *Oncogene* 2004;23:1153–65.
- [24] Pietersen AM, van der Eb MM, Rademaker HJ, van den Wollenberg DJ, Rabelink MJ, Kuppen PJ, et al. Specific tumor-cell killing with adenovirus vectors containing the apoptin gene. *Gene Ther* 1999;6:882–92.
- [25] Zhuang SM, Landegent JE, Verschuere CA, Falkenburg JH, van Ormondt H, van der Eb AJ, et al. Apoptin, a protein encoded by chicken anemia virus, induces cell death in various human hematologic malignant cells in vitro. *Leukemia* 1995;9(Suppl 1):S118–20.
- [26] Zhang Y, Toh L, Lau P, Wang X. Human telomerase reverse transcriptase (hTERT) is a novel target of the Wnt/beta-catenin pathway in human cancer. *J Biol Chem* 2012;287:32494–511.
- [27] Lewis KA, Tollefsbol TO. Regulation of the telomerase reverse transcriptase subunit through epigenetic mechanisms. *Front Genet* 2016;7:83.
- [28] Ramlee MK, Wang J, Toh WX, Li S. Transcription Regulation of the Human Telomerase Reverse Transcriptase (hTERT) gene. *Genes (Basel)* 2016; 7.:pii: E50.
- [29] Sitaram RT, Degerman S, Ljungberg B, Andersson E, Oji Y, Sugiyama H, et al. Wilms' tumour 1 can suppress hTERT gene expression and telomerase activity in clear cell renal cell carcinoma via multiple pathways. *Br J Cancer* 2010;103:1255–62.
- [30] Li X, Liu Y, Wen Z, Li C, Lu H, Tian M, et al. Potent anti-tumor effects of a dual specific oncolytic adenovirus expressing apoptin in vitro and in vivo. *Mol Cancer* 2010;9:10.
- [31] Liu L, Wu W, Zhu G, Liu L, Guan G, Li X, et al. Therapeutic efficacy of an hTERT promoter-driven oncolytic adenovirus that expresses apoptin in gastric carcinoma. *Int J Mol Med* 2012;30:747–54.
- [32] Zhang M, Wang J, Li C, Hu N, Wang K, Ji H, et al. Potent growth-inhibitory effect of a dual cancer-specific oncolytic adenovirus expressing apoptin on prostate carcinoma. *Int J Oncol* 2013;42:1052–60.
- [33] Qi Y, Guo H, Hu N, He D, Zhang S, Chu Y, et al. Preclinical pharmacology and toxicology study of Ad-hTERT-E1a-Apoptin, a novel dual cancer-specific oncolytic adenovirus. *Toxicol Appl Pharmacol* 2014;280:362–9.
- [34] Yang G, Meng X, Sun L, Hu N, Jiang S, Sheng Y, et al. Antitumor effects of a dual cancer-specific oncolytic adenovirus on colorectal cancer in vitro and in vivo. *Exp Ther Med* 2015;9:327–34.
- [35] Sun LL, Jin NY, Xiao L. [Anti-tumor effects of apoptin gene on human laryngeal carcinoma Hep-2]. *Zhonghua Er Bi Yan Hou Tou Jing Wai Ke Za Zhi* 2007;42:148–50.
- [36] Umar A, Dunn BK, Greenwald P. Future directions in cancer prevention. *Nat Rev Cancer* 2012;12:835–48.
- [37] Floor SL, Dumont JE, Maenhaut C, Raspe E. Hallmarks of cancer: of all cancer cells, all the time? *Trends Mol Med* 2012;18:509–15.
- [38] Hanahan D, Weinberg RA. Hallmarks of cancer: the next generation. *Cell* 2011;144:646–74.
- [39] Hu JC, Coffin RS, Davis CJ, Graham NJ, Groves N, Guest PJ, et al. A phase I study of OncoVEXGM-CSF, a second-generation oncolytic herpes simplex virus expressing granulocyte macrophage colony-stimulating factor. *Clin Cancer Res* 2006;12:6737–47.
- [40] Roura S, Galvez-Monton C, Bayes-Genis A. Bioluminescence imaging: a shining future for cardiac regeneration. *J Cell Mol Med* 2013;17:693–703.
- [41] Fujii H, Noda K, Asami Y, Kuroda A, Sakata M, Tokida A. Increase in bioluminescence intensity of firefly luciferase using genetic modification. *Anal Biochem* 2007;366:131–6.
- [42] Marques SM, Esteves da Silva JC. Firefly bioluminescence: a mechanistic approach of luciferase catalyzed reactions. *IUBMB Life* 2009;61:6–17.
- [43] Adams ST Jr., Miller SC. Beyond D-luciferin: expanding the scope of bioluminescence imaging in vivo. *Curr Opin Chem Biol* 2014;21:112–20.
- [44] Evans MS, Charette JP, Adams ST Jr., Reddy GR, Paley MA, Aroinin N, et al. A synthetic luciferin improves bioluminescence imaging in live mice. *Nat Methods* 2014;11:393–5.
- [45] Demirtas L, Guclu A, Erdur FM, Akbas EM, Ozcicek A, Onk D, et al. Apoptosis, autophagy & endoplasmic reticulum stress in diabetes mellitus. *Indian J Med Res* 2016;144:515–24.
- [46] Maddika S, Mendoza FJ, Hauff K, Zamzow CR, Paranjothy T, Los M. Cancer-selective therapy of the future: apoptin and its mechanism of action. *Cancer Biol Ther* 2006;5:10–9.
- [47] Singh PK, Tiwari AK, Rajmani RS, Kumar GR, Chaturvedi U, Saxena L, et al. Apoptin as a potential viral gene oncotherapeutic agent. *Appl Biochem Biotechnol* 2015;176:196–212.
- [48] Bullenkamp J, Gaken J, Festy F, Chong EZ, Ng T, Tavassoli M. Apoptin interacts with and regulates the activity of protein kinase C beta in cancer cells. *Apoptosis* 2015;20:831–42.
- [49] Li X, Jin N, Mi Z, Lian H, Sun L, Li X, et al. Antitumor effects of a recombinant fowlpox virus expressing Apoptin in vivo and in vitro. *Int J Cancer* 2006;119:2948–57.

- [50] Pan Y, Fang L, Fan H, Luo R, Zhao Q, Chen H, et al. Antitumor effects of a recombinant pseudotype baculovirus expressing Apoptin in vitro and in vivo. *Int J Cancer* 2010;126:2741–51.
- [51] Jin JL, Gong J, Yin TJ, Lu YJ, Xia JJ, Xie YY, et al. PTD4-apoptin protein and dacarbazine show a synergistic antitumor effect on B16-F1 melanoma in vitro and in vivo. *Eur J Pharmacol* 2011;654:17–25.
- [52] Danen-Van Oorschot AA, Zhang YH, Leliveld SR, Rohn JL, Seelen MC, Bolk MW, et al. Importance of nuclear localization of apoptin for tumor-specific induction of apoptosis. *J Biol Chem* 2003;278:27729–36.
- [53] Kuusisto HV, Wagstaff KM, Alvisi G, Jans DA. The C-terminus of apoptin represents a unique tumor cell-enhanced nuclear targeting module. *Int J Cancer* 2008;123:2965–9.
- [54] Wadia JS, Wagner MV, Ezhevsky SA, Dowdy SF. Apoptin/VP3 contains a concentration-dependent nuclear localization signal (NLS), not a tumorigenic selective NLS. *J Virol* 2004;78:6077–8.
- [55] Doloff JC, Waxman DJ. Adenoviral vectors for prodrug activation-based gene therapy for cancer. *Anticancer Agents Med Chem* 2014;14:115–26.